

α -Benzithiazolyl 3-Pyrrolyl BODIPY Probe for Ratiometric Selective Sensing of Cyanide ion and Bioimaging Studies

Kanhu Charan Behera^a, Roshnara Mohanty^b, Mangalampalli Ravikanth^{a*}

^aDepartment of Chemistry, Indian Institute of Technology Bombay, Powai, Mumbai 400076, India. E-mail: ravikanth@chem.iitb.ac.in

^bCSIR - National Environmental Engineering Research Institute, Chennai Zonal Laboratory, Chennai - 600113, India

Supplementary information

Sl. no	Details	Page no.
1.	Experimental: Materials and methods	S2-S4
2.	Characterization data of compounds 3 and 3-CN	S4-S8
3.	X-ray crystal data of 3	S9-S11
4.	Photophysical investigations: Photophysical data of 3 and 3-CN Excited state life time data (TCSPC measurements) of 3 and 3-CN	S11-S13
	Theoretical calculations: DFT optimized structure and data of 3 and 3-CN and TD-DFT data	S14-S20
7.	References	S20

MATERIALS AND METHODS

Materials:

The chemicals, such as $\text{BF}_3 \cdot \text{Et}_2\text{O}$ and 2,3-dichloro-5,6-dicyano-1,4-benzoquinone (DDQ), hydrazine hydrate, TFA, DMF, 2-aminothiophenol, NaCN, POCl_3 and tetrabutyl ammonium salt of various anions were used as obtained from Aldrich and TCI. All other chemicals used for the synthesis were reagent grade unless otherwise specified. Column chromatography was performed on silica gel (100-200) and basic alumina.

Methods:

- The ^1H and ^{13}C NMR spectra were recorded in CDCl_3 on Bruker 400 and 500 MHz instruments. The frequencies for the ^{13}C nucleus are 100.06 and 125.77 MHz for 400 and 500 MHz instruments, respectively. Similarly, the frequencies for the ^{11}B and ^{19}F nucleus are 193 and 376 MHz for 400 MHz instruments.
- Absorption and steady state fluorescence spectra were obtained with PerkinElmer Lambda-35.
- Cyclic voltammetry (CV) studies were carried out with the BAS electrochemical system utilizing the three-electrode configuration consisting of glassy carbon (working electrode), platinum wire (auxiliary electrode), and saturated calomel (reference electrode) electrodes. The experiments were done in dry dichloromethane using tetrabutylammonium perchlorate as a supporting electrolyte.
- Mass spectra were recorded with a Q-TOF micro mass spectrometer.
- Fluorescence quantum yields were determined^{S1} in each case by comparing the corrected spectrum with that of Rhodamine 6G ($\Phi = 0.95$)^{S2} in EtOH by taking the area under total emission using the procedure reported earlier.

- The exponential decay curve of **3** and **3-CN** were fitted appropriately with a mono/bi-exponential equation $Y = A + B_1 \exp(-t/\tau_1) + B_2 \exp(-t/\tau_2)$ to obtain best goodness-of-fit χ^2 value. The average life time (τ_{av}) was calculated following the equations depicted in literature^{S3}.
- Rigaku Saturn 724 diffractometer was used for performing Single-crystal X-ray structure analysis which comprised of a low-temperature attachment. Data were collected at 100 K using graphite-monochromated MoK $_{\alpha}$ radiation (λ_{α} = 0.71073 Å) by the ω -scan technique. Data were reduced by using Crystal Clear-SM Expert 2.1 b24 software. Structures were solved by direct methods and refined by least-squares against F2 utilizing the software packages SHELXL-97, SIR-92 and WINGX. All non-hydrogen atoms were refined anisotropically. X-ray data for the compound **3** was collected on a Bruker Kappa CCD diffractometer equipped with a graphite monochromated MoK $_{\alpha}$ radiation source at 200 K using the θ -2 θ scan mode.
- Quantum chemical calculations (gas phase/vacuum) for ground state energy minimized structures for the probes **3** and **3-CN** were done employing density functional theory (DFT) in a Gaussian 09W program package. The ground state structural elucidation involved in optimization using DFT based Beck-3 Lee Young Parr (B3LYP) functional where 6-31+G(d,p) basis sets were used. To obtain the oscillator strengths, identical basis and functional hybrid set were used whereas the vertical excitation energies were obtained with the help of TD-DFT techniques. Under the Polarisable Continuum Model (PCM) in the CH₂Cl₂ media, TD-DFT analysis were done using the Self-Consistent Reaction Field (SCRF). The electronic absorption spectra as well as the oscillator strengths were thoroughly examined using TD-DFT with PCM model on the basis of the optimized structures in the S₀ state. The natural bond orbital (NBO) study of the title molecule **3** and **3-CN** was computed at the

B3LYP/6-31g level of the model. Second-order perturbation theory, applied to the Fock matrix, was utilized to evaluate donor-acceptor interactions in the NBO investigation. The strength of interaction stabilization energy $E^{(2)}$, indicative of electron delocalization between the donor (i) and acceptor (j) ($i \rightarrow j$), was assessed using the following below equation

$$E^{(2)} = \Delta E_{ij} = q_i \frac{F(i, j)^2}{\epsilon_j - \epsilon_i}$$

where q_i is the donor orbital occupancy, $F(i, j)$ is the off-diagonal NBO Fock matrix element, and ϵ_j and ϵ_i are implies diagonal elements (orbital energies).

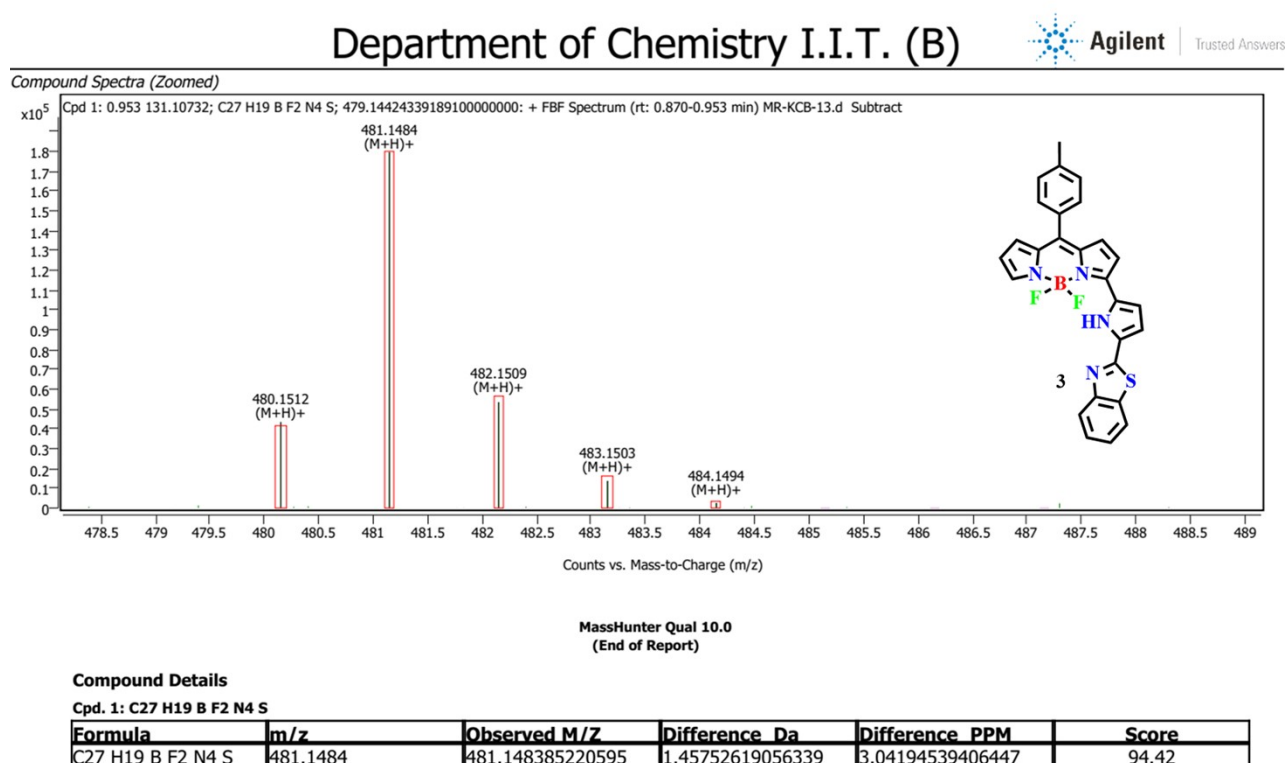


Fig. S1. HR-MS of compound 3.

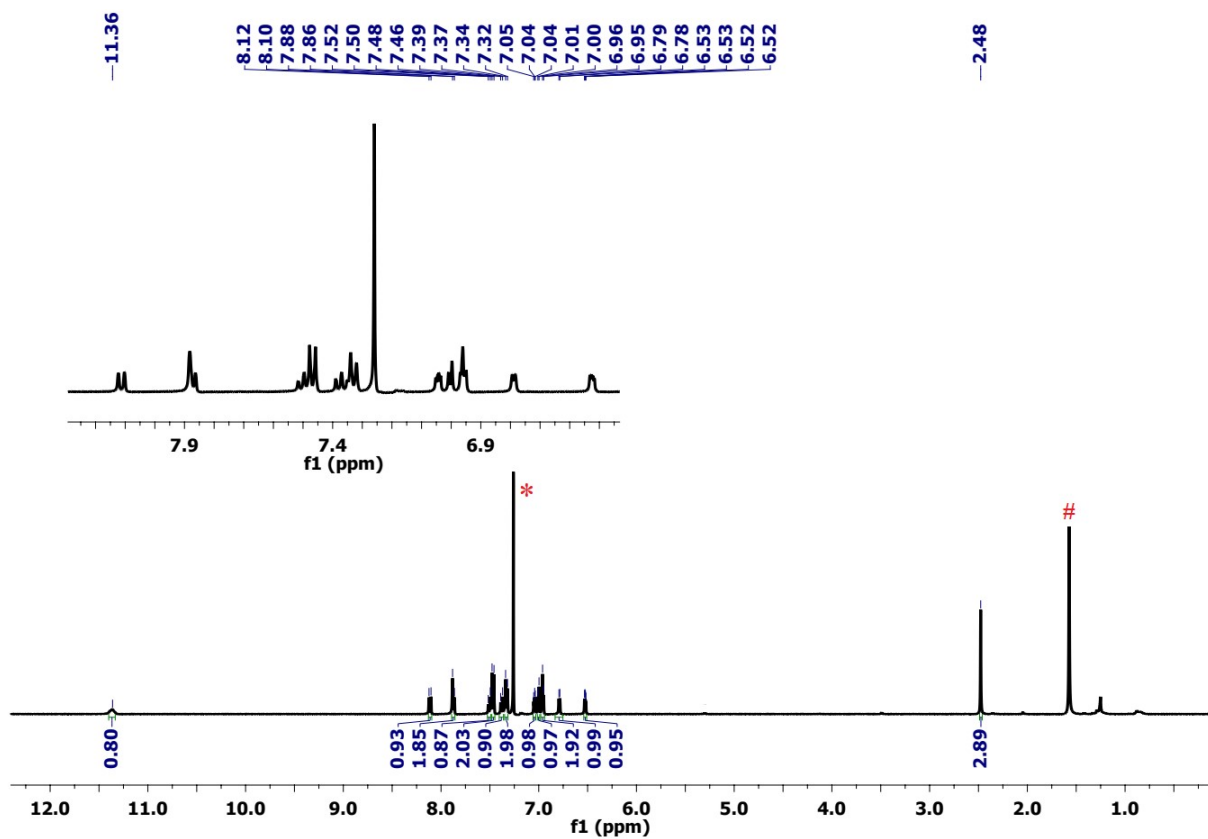


Fig. S2. ^1H NMR spectrum of **3** in CDCl_3 at room temperature.

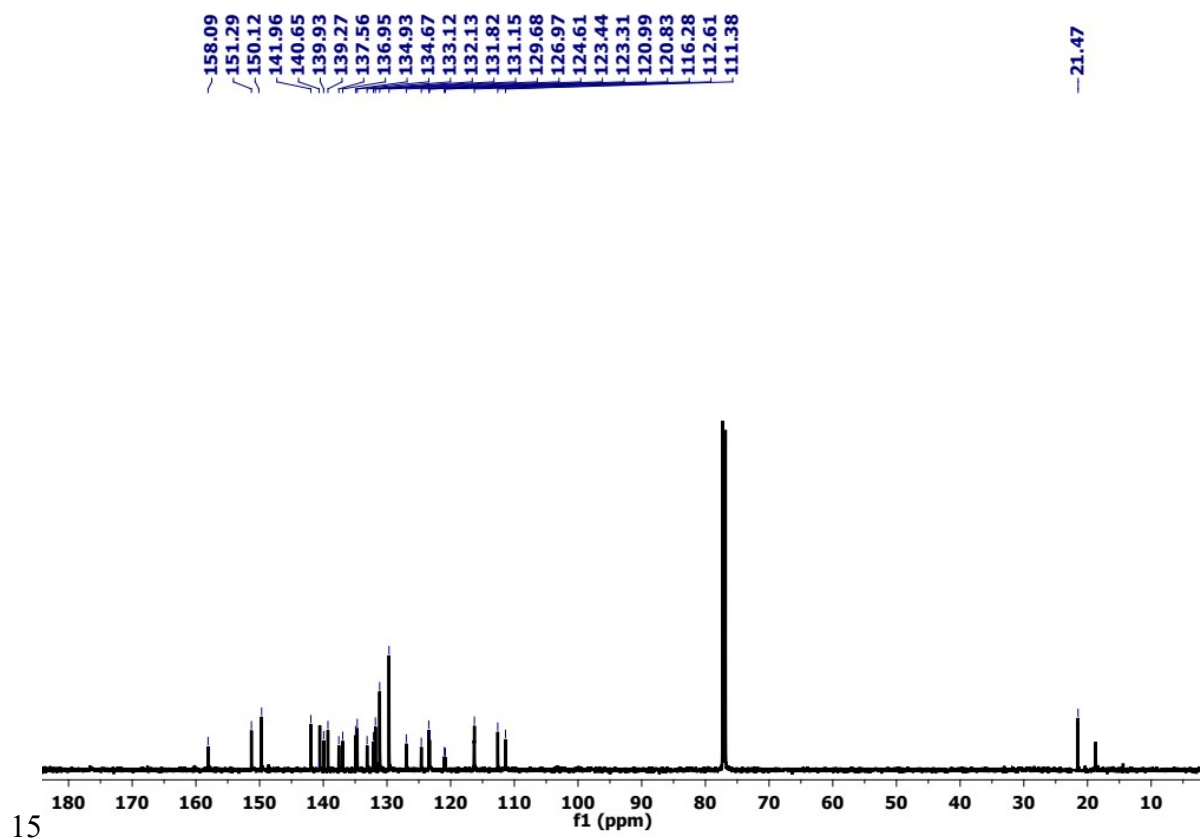


Fig. S3. ^{13}C NMR spectrum of **3** in CDCl_3 at room temperature.

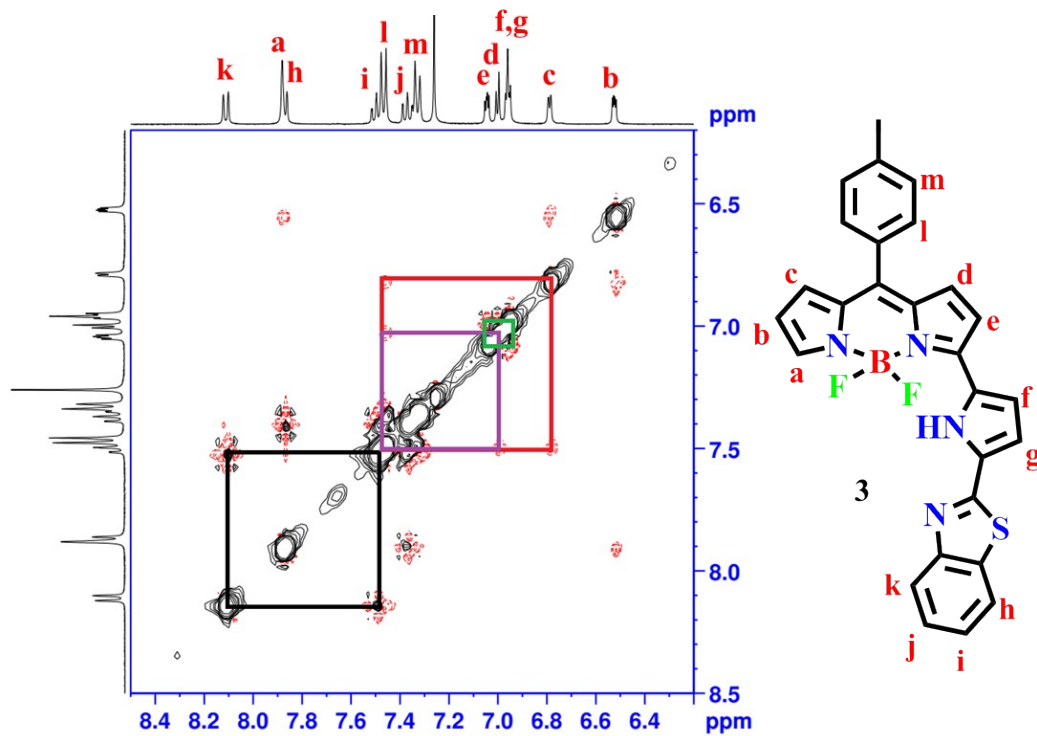


Fig. S4. ^1H - ^1H NOESY spectrum of the **3** in CDCl_3 at room temperature.

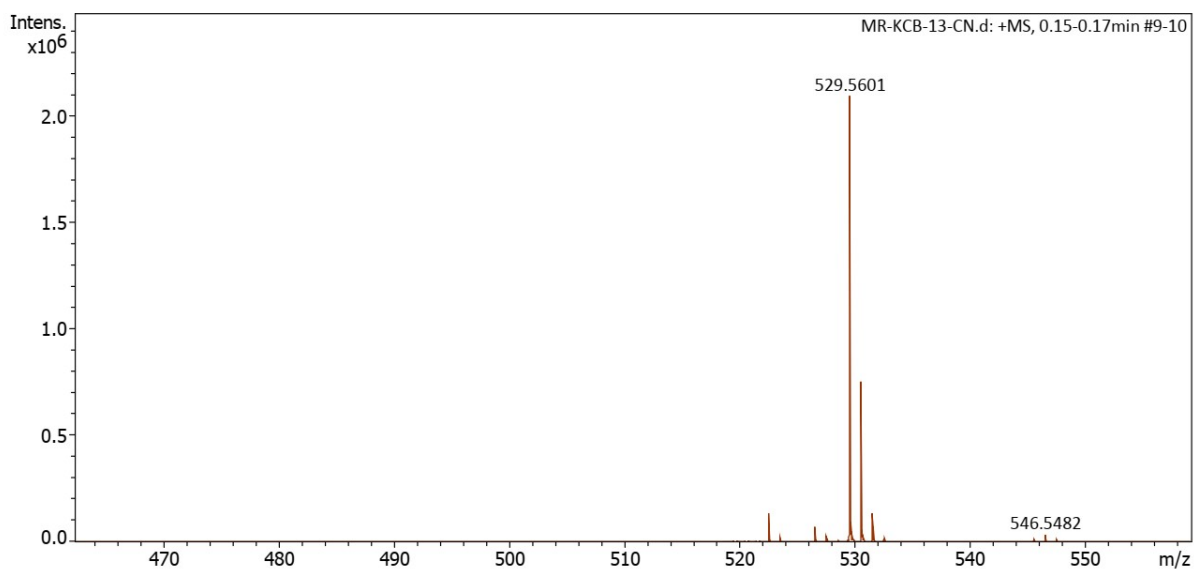


Fig. S5. HR-MS of compound **3-CN**.

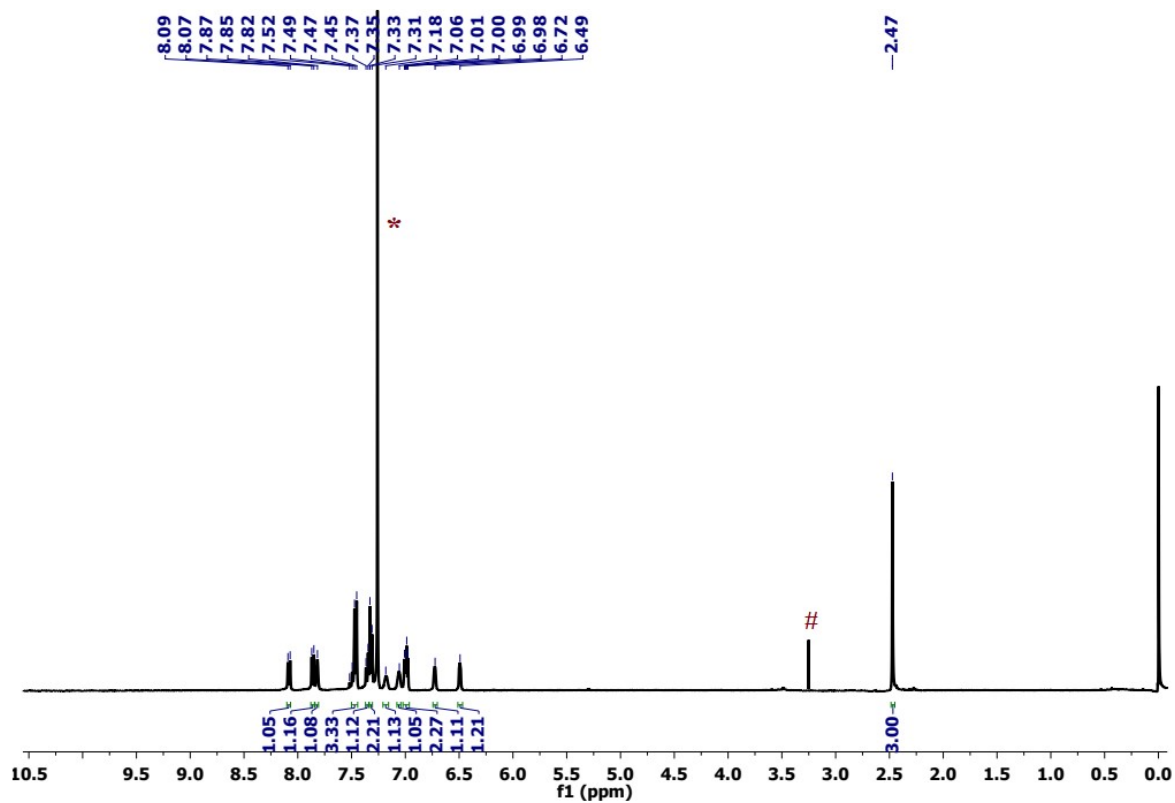


Fig. S6. ^1H NMR spectrum of **3-CN** in CDCl_3 at room temperature.

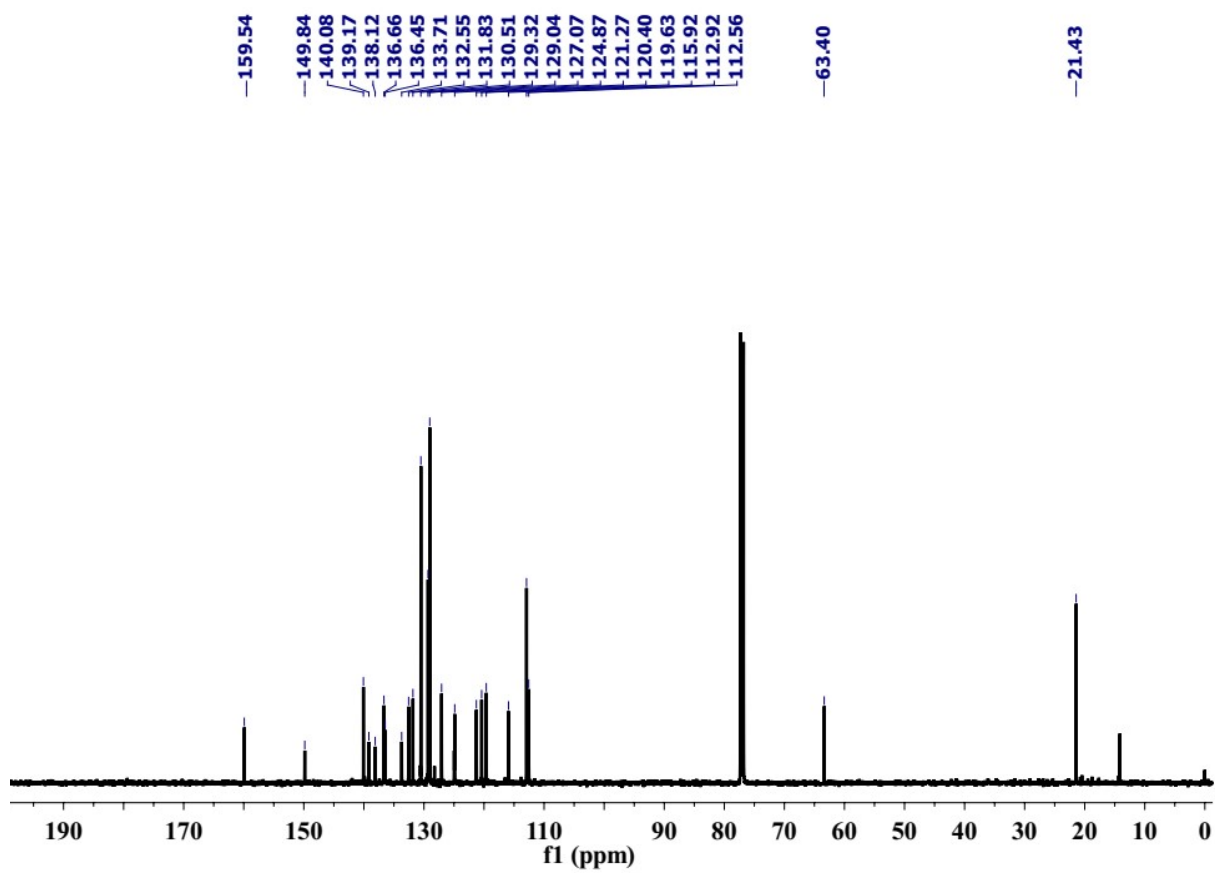


Fig. S7. ^{13}C NMR spectrum of **3-CN** in CDCl_3 at room temperature.

Table S1 Crystallographic parameters and structure refinement of structure of compound **3**.

<i>Empirical formula</i>	C₂₇H₁₉BF₂N₄S
<i>Formula weight</i>	480.33
<i>Temperature/K</i>	106(8)
<i>Crystal system</i>	monoclinic
<i>Space group</i>	C2/c
<i>a/Å</i>	19.5653(3)
<i>b/Å</i>	16.6631(2)
<i>c/Å</i>	14.1015(2)
<i>α/°</i>	90
<i>β/°</i>	107.245(2)
<i>γ/°</i>	90
<i>Volume/Å³</i>	4390.68(12)
<i>Z</i>	8
<i>ρ_{calc}/cm³</i>	1.453
<i>μ/mm⁻¹</i>	0.190
<i>F(000)</i>	1984.0
<i>Crystal size/mm³</i>	0.12 × 0.11 × 0.011
<i>Radiation</i>	Mo Kα (λ = 0.71073)
<i>2θ range for data collection/°</i>	3.274 to 50
<i>Index ranges</i>	-23 ≤ h ≤ 23, -19 ≤ k ≤ 19, -16 ≤ l ≤ 16
<i>Reflections collected</i>	54489
<i>Independent reflections</i>	3845 [R_{int} = 0.1591, R_{sigma} = 0.0682]
<i>Data/restraints/parameters</i>	3845/0/317
<i>Goodness-of-fit on F²</i>	1.070
<i>Final R indexes [I > 2σ (I)]</i>	R₁ = 0.0348, wR₂ = 0.0940
<i>Final R indexes [all data]</i>	R₁ = 0.0382, wR₂ = 0.0962
<i>Largest diff. peak/hole / e Å⁻³</i>	0.32/-0.31

Table S2. Bond Lengths for compound 3

Atom	Atom	Length/Å	Atom	Atom	Length/Å
S1	C14	1.7475(14)	C9	C8	1.4226(19)
S1	C15	1.7283(15)	C9	C10	1.436(2)
F1	B1	1.4003(19)	C10	C11	1.398(2)
F2	B1	1.3949(18)	C11	C12	1.399(2)
N1	C1	1.3538(18)	C13	C12	1.388(2)
N1	C4	1.3868(18)	C13	C14	1.446(2)
N1	B1	1.529(2)	C16	C15	1.401(2)
N2	C6	1.4044(17)	C16	C17	1.372(2)
N2	C9	1.3607(18)	C18	C17	1.402(2)
N2	B1	1.5485(18)	C19	C18	1.383(2)
N3	C10	1.3717(18)	C19	C20	1.397(2)
N3	C13	1.3613(18)	C20	C15	1.410(2)
N4	C14	1.3048(18)	C21	C5	1.4865(19)
N4	C20	1.3910(19)	C22	C21	1.396(2)
C1	C2	1.388(2)	C22	C23	1.392(2)
C3	C2	1.389(2)	C24	C23	1.395(2)
C4	C3	1.404(2)	C24	C25	1.395(2)
C4	C5	1.4145(19)	C24	C27	1.5057(19)
C5	C6	1.389(2)	C26	C21	1.400(2)
C6	C7	1.4207(19)	C26	C25	1.386(2)
C8	C7	1.365(2)			

Table S3. Bond Angles for compound 3

Atom	Atom	Atom	Angle/°	Atom	Atom	Atom	Angle/°
C15	S1	C14	88.78(7)	N3	C13	C14	120.02(13)
C1	N1	C4	107.80(12)	C12	C13	C14	131.62(13)
C1	N1	B1	126.22(12)	N4	C14	S1	116.53(11)
C4	N1	B1	125.96(11)	N4	C14	C13	123.44(13)
C6	N2	B1	123.86(11)	C13	C14	S1	119.88(11)
C9	N2	C6	107.69(11)	C16	C15	S1	128.58(12)
C9	N2	B1	128.18(12)	C16	C15	C20	121.63(14)
C13	N3	C10	109.94(12)	C20	C15	S1	109.78(11)
C14	N4	C20	109.98(12)	C17	C16	C15	117.73(14)
N1	C1	C2	109.79(13)	C16	C17	C18	121.32(14)
C1	C2	C3	107.20(13)	C19	C18	C17	121.20(15)
C2	C3	C4	107.18(13)	C18	C19	C20	118.62(14)
N1	C4	C3	108.01(12)	N4	C20	C15	114.92(13)
N1	C4	C5	120.26(13)	N4	C20	C19	125.59(13)
C3	C4	C5	131.57(13)	C19	C20	C15	119.48(13)
C4	C5	C21	118.54(12)	C22	C21	C5	123.25(13)
C6	C5	C4	120.11(12)	C22	C21	C26	118.35(13)
C6	C5	C21	121.23(12)	C26	C21	C5	118.39(12)
N2	C6	C7	107.78(12)	C23	C22	C21	120.43(13)
C5	C6	N2	121.61(12)	C22	C23	C24	121.29(13)

C5	C6	C7	130.57(13)	C23	C24	C25	117.98(13)
C8	C7	C6	107.75(12)	C23	C24	C27	121.49(13)
C7	C8	C9	107.79(12)	C25	C24	C27	120.53(13)
N2	C9	C8	108.98(12)	C26	C25	C24	121.12(13)
N2	C9	C10	127.49(12)	C25	C26	C21	120.81(13)
C8	C9	C10	123.50(12)	F1	B1	N1	111.04(12)
N3	C10	C9	126.34(12)	F1	B1	N2	109.63(12)
N3	C10	C11	106.81(12)	F2	B1	F1	108.01(12)
C11	C10	C9	126.76(13)	F2	B1	N1	110.05(12)
C10	C11	C12	108.01(13)	F2	B1	N2	110.61(12)
C13	C12	C11	107.05(13)	N1	B1	N2	107.51(11)
N3	C13	C12	108.18(12)				

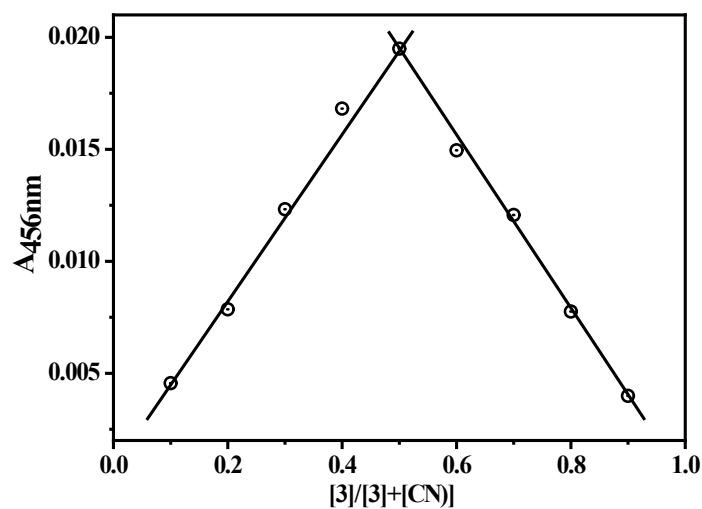


Fig. S8. Job's plot of **3** in the presence of CN⁻.

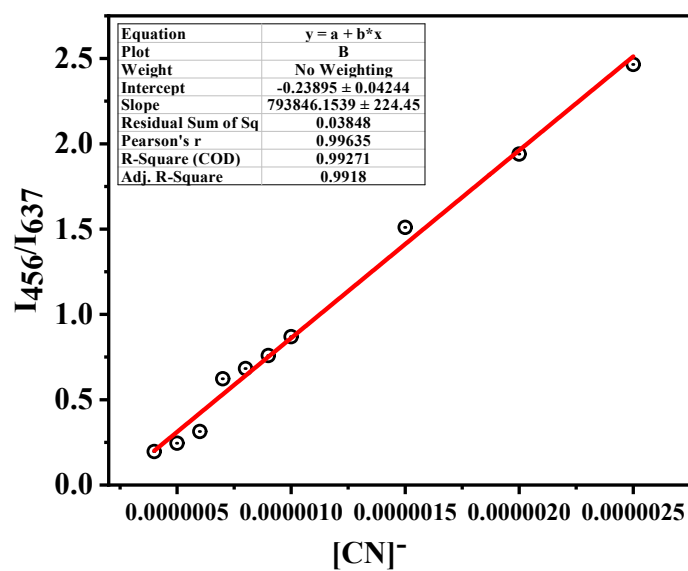


Fig.S9. Linear regressions of the plot of fluorescence spectral intensity ratio $[(I_{456}/I_{637})]$ of **3** with CN^- at lower concentration level for determination of sensitivity of detection ($S/N = 5$). *Conditions*, Fluo.: $[\mathbf{3}] = 1\ \mu\text{M}$, RT, $\lambda_{\text{ex}} = 400\ \text{nm}$, em. /ex. b. p.=5 nm

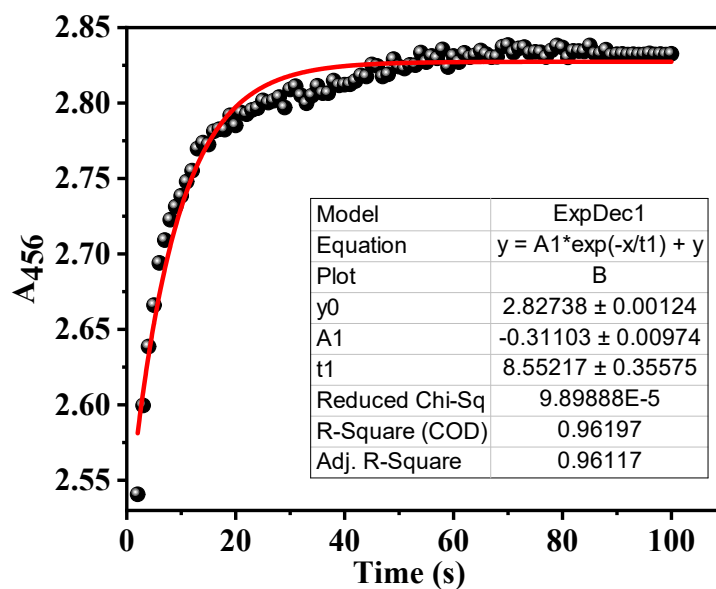


Fig. S10. Rate constant calculation from the absorbance profile of **3** ($[\mathbf{3}] = 100\ \mu\text{M}$) in the presence of CN^- in 1:1 ratio stoichiometry as a function of time.

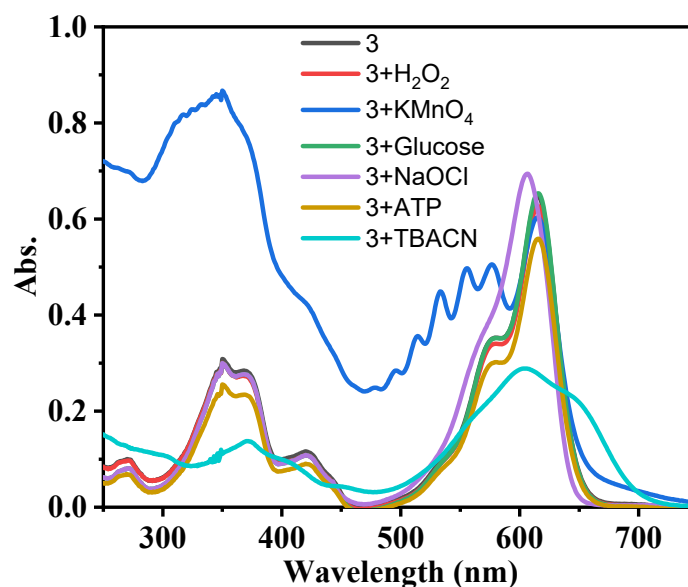


Fig. S11. Absorbance profile of **3** in the presence of some oxidizing agents. *Conditions*: $[\mathbf{3}] = 10\ \mu\text{M}$ and $[\text{oxidising agent}] = 100\ \mu\text{M}$.

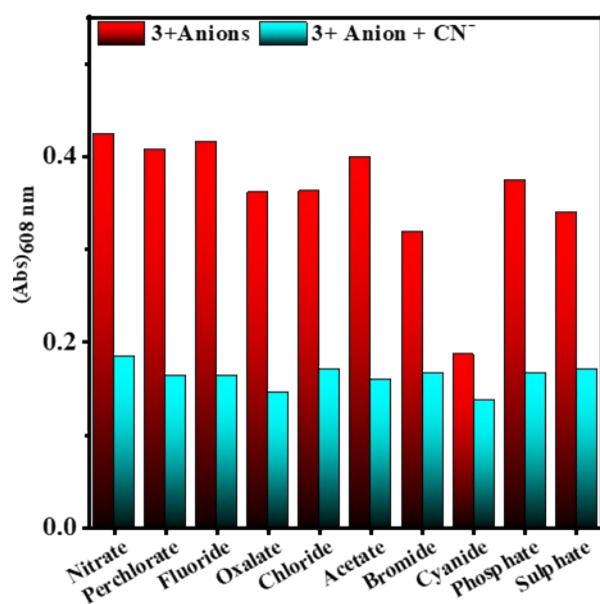


Fig. S12. The bar diagram to the Absorbance at 608 nm of **3** with various anions used in this study (red colored bar); subsequent addition of CN⁻ (sky colored bar).

Table S4: Fit-results to the exponential decay curve of **3** with and without CN obtained with time-correlated single photon counting technique with exponential fit equation $A+B_1 \exp(-t/\tau_1) + B_2 \exp(-t/\tau_2)$.

<i>Parameter</i>	3, $\lambda_{ex.}=400$ nm		3-CN, $\lambda_{ex.}=400$ nm	
	$\lambda_{em.}=456$ nm	$\lambda_{em.}=637$ nm	$\lambda_{em.}=456$ nm	$\lambda_{em.}=637$ nm
τ_1 , ns (%)	0.95 (86.24)	4.43 (100)	0.98 (8.16)	1.41 (22.65)
τ_2 , ns (%)	3.22 (13.76)		2.05 (91.84)	3.45 (77.35)
τ_{av} , ns	1.02	4.43	1.89	1.53
χ^2	1.24	1.02	1.02	1.12

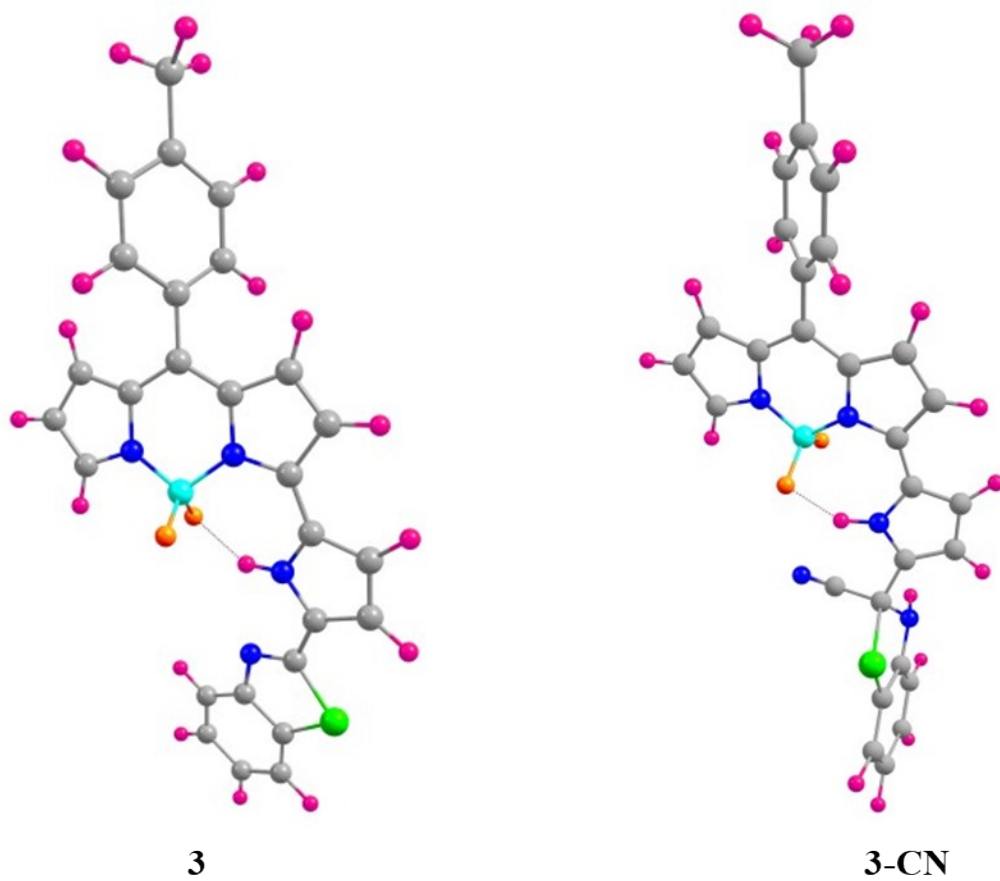


Fig. S13. DFT Optimized structures of **3** and **3-CN**.

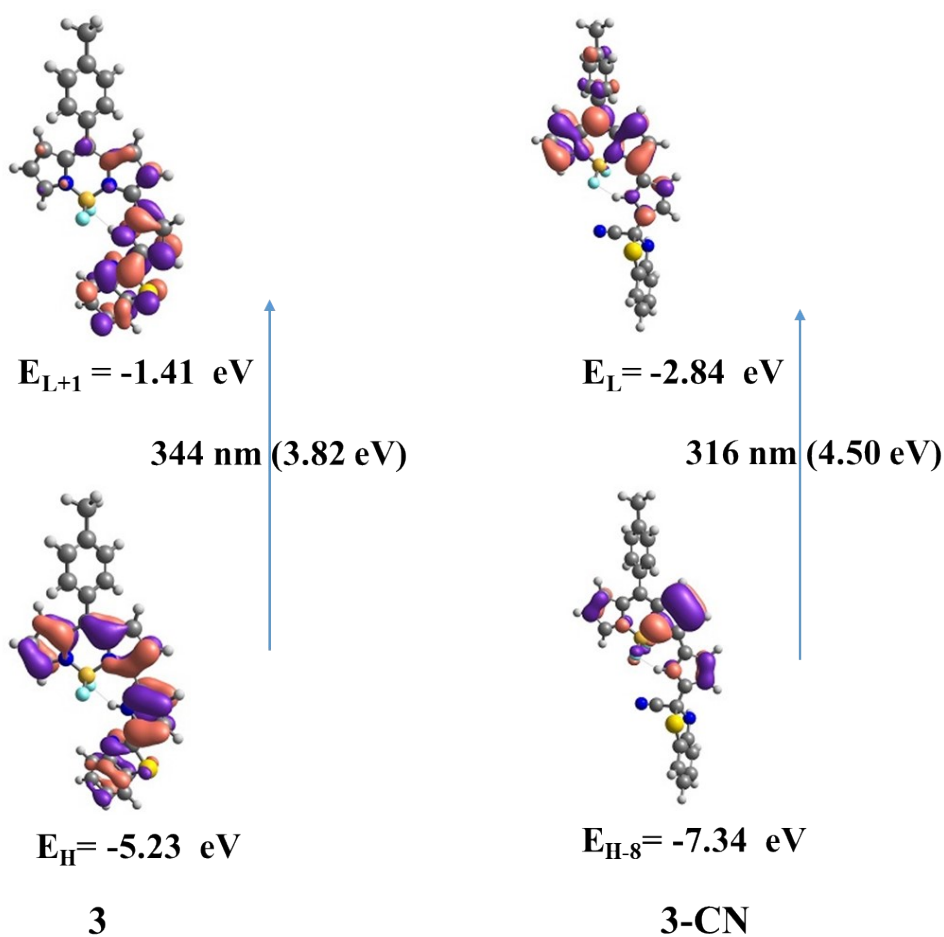


Fig. S14. FMO diagram of H \rightarrow L+1 for **3** and the H-8 \rightarrow L for **3-CN**.

Table S5. S_0 optimized geometry of the compound **3** at B3LYP/6-31g (d,p) level of theory #
 Total Energy (Hartree) = -1881.959614

Atom	X	Y	Z	Atom	X	Y	Z
S	-5.869292000	-1.654387000	0.205006000	F	-0.083769000	0.832545000	1.670594000
F	-0.445715000	1.189956000	-0.556043000	N	-1.837290000	-1.072302000	0.033032000
H	-1.694848000	-0.095295000	-0.210920000	N	1.170415000	-0.520399000	0.105796000
N	1.651223000	1.912546000	0.363892000	N	-4.268966000	0.373227000	-0.269665000
C	5.389258000	-0.777532000	-1.144035000	H	4.684844000	-1.226987000	-1.835732000
C	7.685218000	-0.417326000	-0.422207000	C	6.755103000	-1.010551000	-1.286677000
H	7.107910000	-1.655244000	-2.087078000	C	9.161033000	-0.696312000	-0.557575000
H	9.476340000	-1.470931000	0.153786000	H	9.754042000	0.199949000	-0.346488000
H	9.406892000	-1.049868000	-1.563706000	C	0.565803000	-1.740613000	0.118106000
C	5.842953000	0.675506000	0.732714000	H	5.486795000	1.321924000	1.527505000
C	7.204977000	0.429794000	0.587599000	H	7.909372000	0.898884000	1.269378000
C	4.910976000	0.070010000	-0.129796000	C	3.003944000	1.655554000	0.177207000

C	3.679872000	2.896336000	0.123778000	H	4.740539000	3.019918000	-0.037120000
C	-0.842834000	-1.998277000	0.203880000	C	3.467852000	0.331477000	0.021275000
C	1.559635000	-2.755171000	0.035046000	H	1.357367000	-3.816159000	0.010849000
C	2.550027000	-0.727858000	0.010603000	C	1.482718000	3.249605000	0.431426000
H	0.495992000	3.671112000	0.564540000	C	-5.897997000	2.191380000	-0.650531000
H	-5.108384000	2.915315000	-0.822812000	C	-1.462838000	-3.234344000	0.458739000
H	-0.944532000	-4.162100000	0.653547000	C	-3.058299000	-1.670776000	0.167610000
C	2.785262000	-2.129083000	-0.025849000	H	3.759446000	-2.590377000	-0.084934000
C	-2.847367000	-3.027881000	0.441664000	H	-3.620580000	-3.764791000	0.609034000
C	-5.557927000	0.860455000	-0.359139000	C	2.720170000	3.895561000	0.292015000
H	2.880469000	4.964567000	0.303924000	C	-4.264254000	-0.899921000	0.014114000
C	-7.937008000	0.267206000	-0.192313000	H	-8.719486000	-0.464042000	-0.017867000
C	-7.240980000	2.546415000	-0.709898000	H	-7.515134000	3.572649000	-0.934146000
C	-8.251676000	1.594318000	-0.483076000	H	-9.293723000	1.894432000	-0.534301000
C	-6.588116000	-0.089373000	-0.132833000	B	0.522006000	0.864328000	0.421805000

Table S6. S₀ optimized geometry of the compound **3-CN** at B3LYP/6-31g (d,p) level of theory # Total Energy (Hartree)= Energy = -1975.354810

Atom	X	Y	Z	Atom	X	Y	Z
C	7.600455000	0.028718000	-0.504346000	C	6.273515000	0.430061000	-0.630494000
C	5.267822000	-0.171565000	0.147053000	C	5.636281000	-1.177505000	1.057554000
C	6.967534000	-1.565862000	1.182978000	C	7.971832000	-0.970987000	0.406435000
C	9.415886000	-1.375838000	0.564434000	C	3.861370000	0.249346000	0.010575000
C	2.842692000	-0.704935000	-0.111353000	C	3.535402000	1.622847000	0.004602000
C	4.329465000	2.773225000	0.215353000	C	3.478442000	3.877916000	0.155093000
C	2.186920000	3.382639000	-0.077385000	N	2.220054000	2.036533000	-0.168636000
N	1.492130000	-0.347860000	-0.195623000	C	0.769411000	-1.490982000	-0.352628000
C	1.653147000	-2.604601000	-0.375519000	C	2.934435000	-2.117804000	-0.232923000
C	-0.657018000	-1.589605000	-0.483821000	N	-1.548857000	-0.582541000	-0.202459000
C	-2.818830000	-1.019177000	-0.437534000	C	-2.760845000	-2.336227000	-0.880668000
C	-1.402352000	-2.697595000	-0.907124000	C	-4.015596000	-0.165720000	-0.178353000
B	0.996511000	1.123002000	-0.368041000	F	0.424484000	1.288044000	-1.621606000
F	0.033765000	1.440343000	0.623362000	N	-5.149719000	-0.573482000	-0.998788000
C	-6.386270000	-0.245329000	-0.421156000	C	-6.339987000	-0.112904000	0.976704000
S	-4.683620000	-0.362355000	1.591136000	C	-7.594631000	-0.109944000	-1.099581000
C	-8.757025000	0.145403000	-0.360739000	C	-8.710797000	0.268295000	1.029287000
C	-7.491796000	0.140990000	1.711002000	C	-3.683602000	1.272757000	-0.368591000
N	-3.432944000	2.393815000	-0.539583000	H	8.361495000	0.491703000	-1.126738000
H	6.000453000	1.192787000	-1.351687000	H	4.874579000	-1.634230000	1.680187000

H	7.234901000	-2.339144000	1.898065000	H	9.919470000	-0.736694000	1.301698000
H	9.959862000	-1.276970000	-0.380568000	H	9.501738000	-2.410216000	0.912267000
H	5.392550000	2.767869000	0.405122000	H	3.744408000	4.918911000	0.274023000
H	1.250317000	3.914599000	-0.171040000	H	1.343085000	-3.635031000	-0.472441000
H	3.855554000	-2.680619000	-0.216917000	H	-1.272125000	0.329798000	0.156331000
H	-3.616383000	-2.937856000	-1.147829000	H	-0.986191000	-3.643565000	-1.222865000
H	-5.036735000	-0.366252000	-1.984839000	H	-7.628231000	-0.202270000	-2.180836000
H	-9.702370000	0.256651000	-0.882674000	H	-9.617601000	0.472955000	1.589193000
H	-7.447468000	0.245799000	2.790271000				

Table S7. Major transitions were calculated using TD-DFT studies of **3**.

Energy (cm-1)	Wavelength (nm)	Osc. Strength	Major contribs
17487.71	571.8	0.9729	HOMO->LUMO (100%)
24658.78	405.5	0.1341	H-1->LUMO (85%), HOMO->L+1 (11%)
25988.79	384.7	0.0197	H-2->LUMO (98%)
26750.18	373.8	0.2857	H-3->LUMO (88%)
27722.08	360.7	0.1496	H-4->LUMO (74%), HOMO->L+1 (23%)
29057.73	344.1	0.4379	H-5->LUMO (16%), H-4->LUMO (20%), H-1->LUMO (10%), HOMO->L+1 (46%)
29469.07	339.3	0.0911	H-5->LUMO (75%)
30132.06	331.8	0.0076	H-7->LUMO (14%), H-6->LUMO (77%)
31024.11	322.3	0.0875	H-7->LUMO (78%), H-6->LUMO (13%)
33060.66	302.4	0.0865	H-8->LUMO (85%)
34694.74	288.2	0.0003	H-9->LUMO (95%)
35272.23	283.5	0.015	HOMO->L+2 (96%)
35335.14	283.0	0.0105	H-2->L+1 (62%), HOMO->L+4 (30%)
35608.57	280.8	0.0053	H-1->L+1 (11%), HOMO->L+3 (86%)
36001.36	277.7	0.0572	H-1->L+1 (77%), HOMO->L+3 (10%)
37855.63	264.1	0.0683	H-2->L+1 (30%), HOMO->L+4 (65%)
38467.80	259.9	0.002	HOMO->L+6 (92%)
39047.71	256.1	0.1363	H-3->L+1 (30%), HOMO->L+5 (55%)
39884.11	250.7	0.0189	H-3->L+1 (63%), HOMO->L+5 (23%)
40751.16	245.4	0.0025	H-10->LUMO (94%)
41176.21	242.8	0.0295	H-11->LUMO (39%), H-6->L+1 (11%), H-4->L+1 (41%)
41419.79	241.4	0.0481	H-11->LUMO (31%), H-4->L+1 (54%)
41827.91	239.0	0.0128	H-11->LUMO (17%), H-6->L+1 (58%)
42501.38	235.2	0.0003	H-9->L+1 (92%)
42565.90	234.9	0.0033	H-5->L+1 (23%), H-5->L+3 (10%), H-3->L+2 (19%), H-1->L+2 (24%)
43485.38	229.9	0.0329	H-7->L+1 (89%)
43574.90	229.4	0.0221	H-8->L+1 (30%), H-5->L+1 (30%), HOMO->L+7 (23%)
43790.25	228.3	0.0129	H-5->L+1 (22%), H-1->L+2 (28%), HOMO->L+7 (20%)
44029.80	227.1	0.0066	H-8->L+1 (18%), H-1->L+3 (43%)
44223.37	226.1	0.0258	H-1->L+2 (10%), H-1->L+3 (12%), H-1->L+4 (22%), HOMO->L+7 (19%)
44806.51	223.1	0.0001	H-2->L+6 (94%)
44900.88	222.7	0.0001	H-13->LUMO (89%)
45107.36	221.6	0.008	H-3->L+2 (25%), H-1->L+2 (21%), H-1->L+3 (24%)

45400.94	220.2	0.046	H-8->L+1 (17%), H-1->L+4 (36%), HOMO->L+7 (18%)
46122.81	216.8	0.0455	H-1->L+5 (19%), HOMO->L+8 (62%)
46876.13	213.3	0.0041	H-2->L+4 (23%), H-1->L+5 (29%), HOMO->L+8 (17%)
47022.92	212.6	0.0073	H-2->L+2 (75%)
47266.50	211.5	0.0038	H-1->L+6 (72%)
47307.64	211.3	0.0099	H-2->L+2 (11%), H-2->L+3 (65%)
47456.04	210.7	0.0005	H-14->LUMO (70%), H-3->L+3 (11%)
47858.52	208.9	0.2154	H-4->L+2 (11%), H-3->L+3 (25%), H-2->L+4 (17%), H-1->L+5 (10%)
48020.63	208.2	0.0013	H-16->LUMO (84%)
48351.32	206.8	0.0003	H-12->LUMO (87%)
48369.06	206.7	0.0594	H-4->L+2 (63%), H-1->L+5 (10%)
48552.15	205.9	0.0127	H-4->L+2 (18%), H-2->L+5 (25%)
48682.81	205.4	0.0266	H-4->L+3 (66%), H-2->L+5 (11%)
48857.84	204.6	0.078	H-4->L+3 (19%), H-3->L+3 (10%), H-2->L+5 (12%)
49134.48	203.5	0.004	H-17->LUMO (94%)
49881.35	200.4	0.1097	H-10->L+1 (18%), H-3->L+4 (45%), H-2->L+5 (16%)
50212.04	199.1	0.0004	H-15->LUMO (72%)

Table S8. Major transitions were calculated using TD-DFT studies of **3-CN**.

Energy (cm-1)	Wavelength (nm)	Osc. Strength	Major contribs
19203.25	546.7	0.8395	HOMO->LUMO (97%)
20275.97	493.1	0.0564	H-1->LUMO (96%)
26043.64	383.9	0.3281	H-3->LUMO (19%), H-2->LUMO (74%)
27030.86	369.9	0.0312	H-3->LUMO (77%), H-2->LUMO (19%)
27923.72	358.1	0.0223	H-4->LUMO (90%)
28835.12	346.8	0.0187	H-1->L+1 (71%), HOMO->L+1 (20%)
29443.26	339.6	0.0081	H-6->LUMO (36%), H-5->LUMO (41%)
29780.40	335.8	0.0575	H-6->LUMO (45%), H-5->LUMO (12%), H-1->L+1 (13%), HOMO->L+1 (26%)
30499.85	327.8	0.0168	H-8->LUMO (23%), H-7->LUMO (28%), H-6->LUMO (12%), HOMO->L+1 (26%)
31103.96	321.5	0.0209	H-8->LUMO (20%), H-7->LUMO (59%)
31548.37	316.9	0.2021	H-8->LUMO (54%), H-5->LUMO (16%), HOMO->L+1 (15%)
36023.94	277.6	0.0145	H-3->L+1 (27%), H-2->L+1 (35%), H-1->L+4 (15%)
36099.76	277.0	0.0161	HOMO->L+2 (71%), HOMO->L+3 (11%)
36176.38	276.4	0.0137	HOMO->L+3 (87%)
37166.83	269.0	0.0485	HOMO->L+4 (77%)
37959.67	263.4	0.0813	H-2->L+1 (11%), H-1->L+2 (19%), H-1->L+4 (44%)
38766.23	257.9	0.2209	H-1->L+6 (45%), HOMO->L+5 (10%), HOMO->L+6 (28%)
39192.09	255.1	0.2033	H-9->LUMO (14%), HOMO->L+5 (65%)
39601.82	252.5	0.0374	H-9->LUMO (44%), HOMO->L+6 (27%)
39720.38	251.7	0.0636	H-9->LUMO (22%), H-1->L+6 (14%), HOMO-

39818.78	251.1	0.0172	>L+6 (29%) H-3->L+1 (21%), H-2->L+1 (22%), H-1->L+2 (22%), H-1->L+5 (12%)
40008.32	249.9	0.0173	H-9->LUMO (14%), H-3->L+1 (22%), H-1->L+2 (19%), H-1->L+5 (14%)
41253.64	242.4	0.0001	H-1->L+3 (97%)
41600.46	240.3	0.0583	H-10->LUMO (85%)
42126.33	237.3	0.0024	H-1->L+2 (16%), H-1->L+4 (15%), H-1->L+5 (63%)
42778.84	233.7	0.002	H-7->L+1 (26%), H-6->L+1 (14%), H-5->L+1 (11%), H-4->L+1 (17%), HOMO->L+7 (22%)
42954.66	232.8	0.007	H-6->L+2 (12%), H-3->L+3 (25%), H-2->L+3 (33%)
43024.03	232.4	0.0003	H-4->L+1 (17%), HOMO->L+7 (67%)
43328.10	230.7	0.0259	H-7->L+1 (18%), H-6->L+1 (10%), H-4->L+1 (57%)
44051.58	227.0	0.0019	H-11->LUMO (95%)
44097.55	226.7	0.0279	H-7->L+1 (18%), H-5->L+1 (59%)
44479.86	224.8	0.0361	H-1->L+7 (58%)
45295.29	220.7	0.0074	H-13->LUMO (44%), H-2->L+2 (37%)
45439.66	220.0	0.0051	H-13->LUMO (49%), H-2->L+2 (32%)
45713.89	218.7	0.0636	H-2->L+4 (15%), H-1->L+8 (48%), HOMO->L+8 (12%)
45749.38	218.5	0.0092	H-8->L+1 (46%), H-6->L+1 (37%)
45959.08	217.5	0.0088	H-8->L+1 (32%), H-7->L+1 (19%), H-6->L+1 (31%)
46134.10	216.7	0.0945	H-2->L+4 (19%), H-2->L+6 (11%), HOMO->L+8 (25%)
46412.36	215.4	0.0083	H-3->L+2 (12%), H-1->L+8 (10%), HOMO->L+8 (46%)
46715.63	214.0	0.1096	H-2->L+5 (14%), H-1->L+8 (15%), HOMO->L+9 (27%)
47139.07	212.1	0.0249	H-3->L+2 (33%), HOMO->L+9 (16%)
47257.63	211.6	0.0174	H-4->L+3 (17%), H-2->L+3 (42%)
47370.55	211.1	0.0425	H-3->L+4 (17%), H-2->L+4 (21%)
47524.60	210.4	0.0365	H-12->LUMO (83%)
47652.84	209.8	0.01	H-15->LUMO (46%), H-2->L+5 (16%)
48117.42	207.8	0.0075	H-15->LUMO (12%), H-4->L+2 (15%), H-2->L+5 (31%), HOMO->L+9 (13%)
48159.36	207.6	0.0102	H-17->LUMO (41%), H-4->L+2 (29%)
48272.28	207.1	0.019	H-17->LUMO (44%), H-4->L+2 (10%)
48306.15	207.0	0.004	H-4->L+3 (48%), H-3->L+3 (21%)
48363.42	206.7	0.0186	H-9->L+1 (13%), H-3->L+4 (23%), H-2->L+6 (33%)

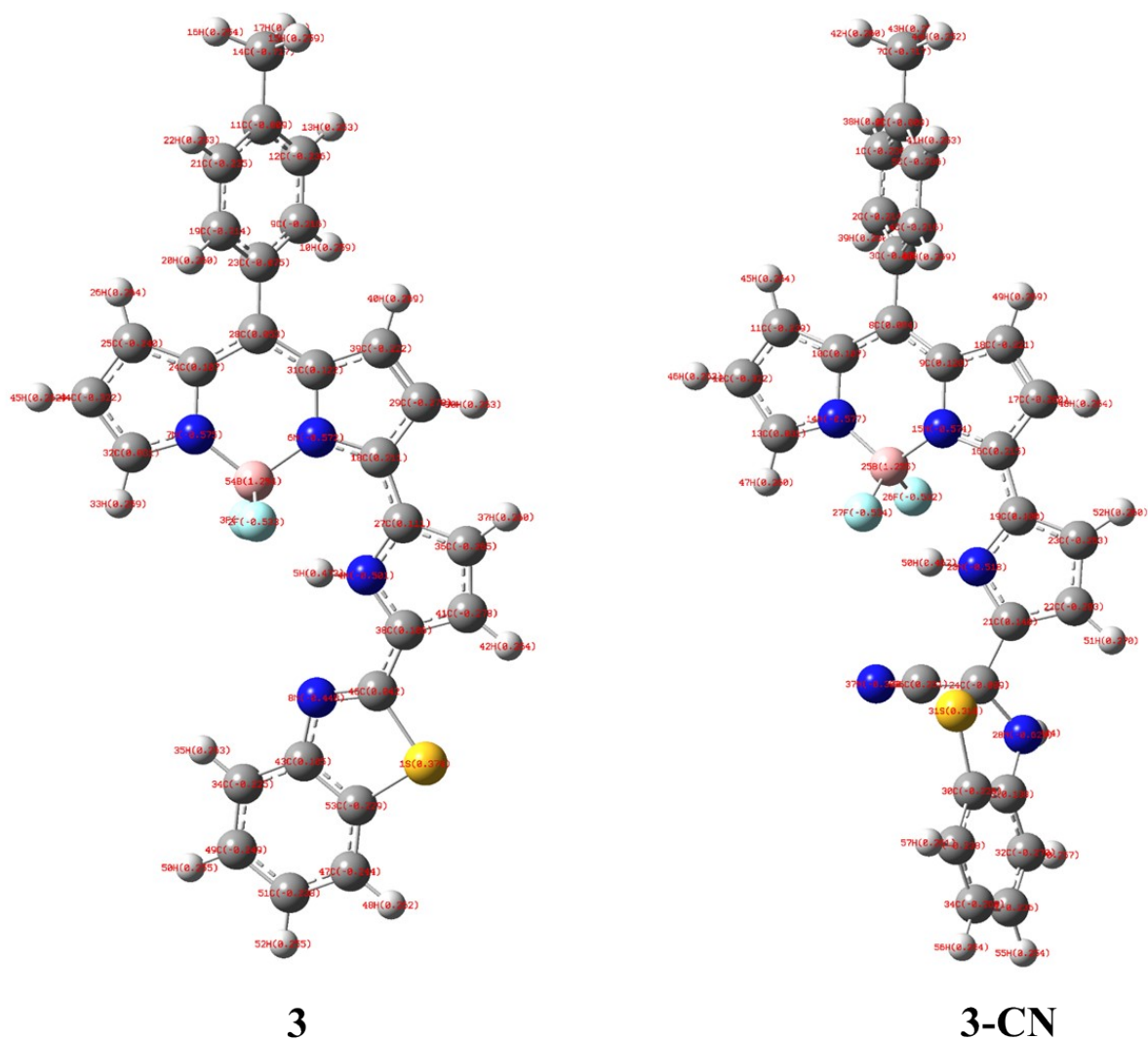


Fig.S15. NBO analysis with charge distribution of **3** and **3-CN**.

References

- S1. M. Fischer and J. Georges, *Chem. Phys. Lett.*, 1996, **260**, 115.
- S2. S. Uchiyama, Y. Matsumura, A. P. de Silva and K. Iwai, *Anal. Chem.*, 2003, **75**, 5926.
- S3. J. R. Lakowicz, *Principles of Fluorescence Spectroscopy*, 3rd edn., Springer Science, 2006, pp. 141-143.